OPTICAL DEEP-SPACE INSTRUMENT FOR NAVIGATION (ODIN)

Ava C. Thrasher[1*], Rebecca Inman[2], Riana Pecourt[2], Ronney Lovelace[2], and Basil Russell-McCorkle[1], John Christian[1]; [1] Space Exploration Analysis Laboratory, Georgia Institute of Technology, 756 W Peachtree St NW, Atlanta, GA 30308 [2]Johnson Space Center. [*][avacthrasher@gatech.edu]

Abstract. *The Optical Deep-Space Instrument for Navigation (ODIN) is a proposed multiple camera, multiple field of view, optical navigation (OPNAV) instrument currently under development. ODIN aims to create a self-sufficient system which can perform imaging target acquisition, star field based attitude estimation, and position estimation using horizon-based OPNAV of known celestial bodies. ODIN will complete these tasks autonomously, thereby contributing to the advancement of OPNAV as an option for truly autonomous mission operations.*

Introduction. Optical navigation (OPNAV) is an established means of spacecraft navigation, with a storied history of enabling missions to the outer planets[1–3] and to small bodies.[4] The promise of OPNAV for enabling autonomous operations was clear immediately, although computing capabilities did not allow meaningful progress in this area until the late 1990s—culminating in the groundbreaking Deep Space 1 mission.[5] Despite some recent advancements demonstrations—notably on Artemis I[6] and OSIRIS-REx,[7] most conventional missions downlink images to Earth for processing and do not make use of autonomous OPNAV. The Optical Deep-Space Instrument for Navigation (ODIN) project aims to develop an integrated sensor system capable of fully autonomous OPNAV anywhere in Earth orbit, lunar orbit, or cislunar space. In this paper we briefly review the initial ODIN design and some of the driving sensor and algorithm challenges.

One of the principle challenges for autonomous OPNAV arises from camera pointing constraints and requirements. Most navigation cameras are narrow field of view (FOV) cameras. Serendipitous imaging aside, these cameras require prior knowledge of the spacecraft's state (both position and orientation) to determine in what direction the instrument must be pointed to acquire the desired OPNAV target. To address this challenge, ODIN proposes design comprised of multiple cameras with mixed FOVs. The system uses wide angle cameras (WACs) cameras for situational awareness and target acquisition, and narrow angle cameras (NACs) for OPNAV measurement generation.

Design Concept. ODIN will be a multiple FOV instrument capable of providing a simultaneous position and attitude estimate at the time of image capture, without requiring any external navigation information (e.g., from the spacecraft). The operational concept to achieve this, as illustrated in Fig. 1, proceeds as follows: First, image processing allows for automated detection and identification of the Earth or Moon in a WAC image. The location of the identified celestial body in the image may be used construct a bearing measurement in the sensor frame. Second, using this bearing measurement, the instrument generates a desired pointing direction which would bring the celestial body into the FOV of a NAC. This does not require knowledge of absolute camera attitude, though in practice this would be known from star field images. The spacecraft then slews to this provided direction. In this orientation simultaneous images are captured using the NACs, where now one is aimed at the celestial body and at least one other is aimed at a star field. The instrument then uses these images to simultaneously perform both position and attitude estimation. A brief review of algorithms needed for this process and their current maturity is given here.

Imaging Target Acquisition. Horizon-based OPNAV requires an image containing a resolved celestial body. Conventionally, prior state knowledge is used to point a NAC at the desired celestial body. To circumvent this, ODIN will use multiple wide FOV cameras (e.g., two 180 degree FOV fisheye cameras mounted opposite of each other), which will be capable of monitoring the majority of the celestial sphere. When a nearby celestial body (i.e., Earth or Moon) is detected, we must convert the pixel coordinates into a line-of-sight (LOS) direction. Doing so requires use of a camera model compatible with large FOV sensors, such as the Scaramuzza model[8] (these are somewhat different from the Brown-Conrady model used for NACs). Once the desired pointing direction is obtained, ODIN will use onboard logic to select one of the NACs to collect the corresponding image.

Attitude Estimation using Star Fields. Attitude estimation from star field images is a straightforward task. Assuming a calibrated camera, this consists of two steps. The first step is to match observed stars to those in a catalog,[9,10] yielding a set of directions (i.e., unit vectors) in correspondence. The second step is to estimate the attitude that best describes the transformation between these two sets of corresponding directions. Given LOS vectors to star observations $\{\boldsymbol{a}_i\}_{i=1}^n$ in the camera frame and the matched catalog stars in the inertial frame $\{\boldsymbol{e}_i\}_{i=1}^n$, the optimal attitude is found as the solution to Wahba's problem[11]

$$\min_{\boldsymbol{T}\in SO(3)} L(\boldsymbol{T}) = \frac{1}{2}\sum_{i=1}^{n} w_i ||\boldsymbol{a}_i - \boldsymbol{T}\boldsymbol{e}_i||^2 \qquad (1)$$

where we seek the attitude transformation matrix $\boldsymbol{T}$ which minimizes the cost function. These measurements can be rewritten as

$$\min_{\boldsymbol{T}\in SO(3)} L(\boldsymbol{T}) = \frac{1}{2}||\boldsymbol{A}\boldsymbol{W}^{\frac{1}{2}} - \boldsymbol{T}\boldsymbol{E}\boldsymbol{W}^{\frac{1}{2}}||_F^2 \qquad (2)$$

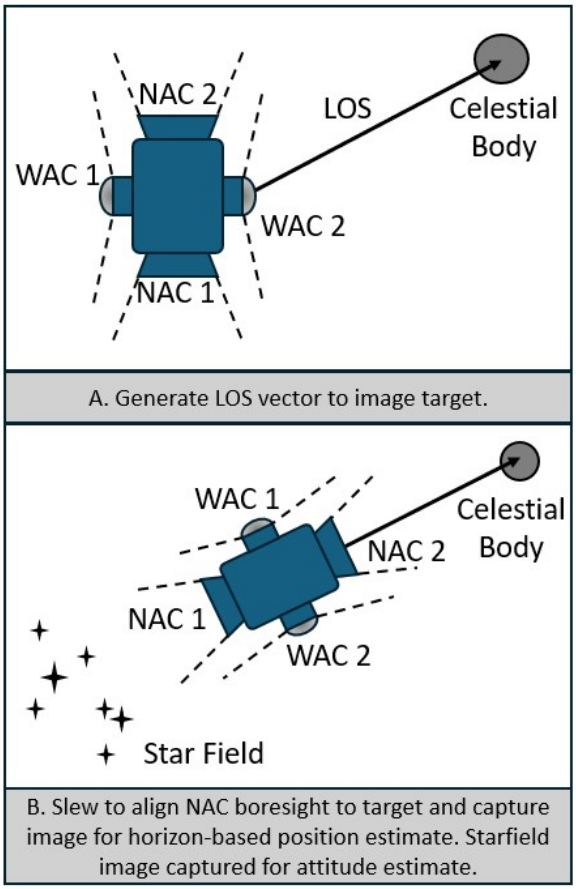

Figure 1. Schematic of a multiple FOV OPNAV instrument. Panel A. a line-of-sight (LOS) vector to an imaging target is acquired using the WAC. Panel B. the spacecraft uses this LOS to determine the necessary slew to align a NAC with the imaging target. Position and attitude estimation are done using the images taken.

where

$$\boldsymbol{A} = [\boldsymbol{a}_1, \boldsymbol{a}_2, \ldots, \boldsymbol{a}_n] \quad \text{and} \quad \boldsymbol{E} = [\boldsymbol{e}_1, \boldsymbol{e}_2, \ldots, \boldsymbol{e}_n] \tag{3}$$

This is the well known orthogonal Procrustes problem. The solution to this problem requires us to first calculate the 3×3 matrix $\boldsymbol{B}$

$$\boldsymbol{B} = (\boldsymbol{A}\boldsymbol{W}^{\frac{1}{2}})(\boldsymbol{E}\boldsymbol{W}^{\frac{1}{2}})^T = \boldsymbol{A}\boldsymbol{W}\boldsymbol{E}^T \tag{4}$$

and then compute the singular value decomposition $\boldsymbol{B} = \boldsymbol{U}\boldsymbol{S}\boldsymbol{V}^T$. The optimal attitude to minimize Wahba's problem is then

$$\tilde{\boldsymbol{T}} = \boldsymbol{U} \begin{bmatrix} 1 & 0 & 0 \\ 0 & 1 & 0 \\ 0 & 0 & det(\boldsymbol{U})det(\boldsymbol{V}) \end{bmatrix} \boldsymbol{V}^T \tag{5}$$

Horizon-Based Position Estimation. ODIN uses horizon-based OPNAV techniques. The horizon is found by performing parallel line scans along the direction of apparent illumination. Candidate horizon points are determined by looking for a persistent jump in image intensity consistent with an extended bright body. The horizon points detected by the line scans are then refined to sub-pixel accuracy using a method based on Zernike moments.[12,13]

ODIN will estimate its position using the Christian-Robinson Algorithm (CRA).[14] This solution provide a non-iterative and exact solution to the problem of horizon-based localization relative to a known ellipsoidal body. This algorithm was also flown as part of the Artemis I OPNAV system.[6]

Current Progress. As the ODIN project works towards developing the first prototype, we completed our first field test in August 2024. The aim of this test was to (1) characterize candidate detectors and lens selections and (2) evaluate our current OPNAV algorithm pipeline.

The field test was completed on August 25th, 2024 in Gilmer County, Georgia, during which 15 star field and 15 Moon images were collected. This test configuration consisted of only a prototype NAC design. Specifically, the sensor used was the FLIR 5 mega-pixel Blackfly S Board Level sensor, and the lens used was the Edmund Optics 25mm C Series fixed focal length lens. Future field tests will include multiple (e.g., WAC+NAC) cameras.

Figure 2. The first imaging field test was completed during which star field and Moon images were captured for camera calibration and initial horizon-based OPNAV techniques were tested.

Camera Calibration and Attitude Estimation. The camera was calibrated using star field images, following the typical procedure[15,16] and making use of the Software for Optical Navigation and Instrument Calibration

(SONIC).[17] Stars in ODIN test images were matched with known stars from the Hipparcos catalog.[18] The Hipparcos catalog is pre-integrated into SONIC. Camera parameters generated from manufacturer-provided specifications, as shown in Table 1, were insufficient to perform star identification using conventional star tracker methods requiring a calibrated camera (e.g., pyramid algorithm[19]). It was, however, quite easy to manually identify a few stars[†] in one image. Given this association, we were able to simultaneously estimate the attitude and focal length, using an algorithm specifically designed for concurrent focal length calibration and attitude estimation.[10]

Table 1. Camera parameters as given by the manufacturers pre-calibration.

Camera Model Parameter	Value
f	25 mm
FPA Resolution	2448x2048
μ	3.45 μm

Once a reasonable estimate of focal length was obtained using the "unknown focal length" algorithm from Ref. [10], the stars in all 15 star field images could be automatically identified using SONIC. These astar correspondences were used to estimate the radial and tangential distortion terms in a five-parameter Brown-Conrady[20,21] distortion model

$$\begin{bmatrix} x_d \\ y_d \end{bmatrix} = (1+k_1 r^2+k_2 r^4+\dots) \begin{bmatrix} x \\ y \end{bmatrix} + \begin{bmatrix} 2p_1 xy + p_2(r^2+2x^2) \\ p_1(r^2+2y^2)+2p_2 xy \end{bmatrix} \tag{6}$$

As is standard practice, we only estimated the parameters k_1, p_1, and p_2. The final estimated focal length and distortion model parameters are shown in Table 2.

Table 2. Camera parameters and distortion model parameters as estimated after the Brown-Conrady model fit.

Camera Model Parameter	Value
f	25.1495 mm
k_1	2.6900e-2
p_1	1.7243e-4
p_2	2.7780e-4

Using the final calibrated camera model and estimated attitude, the Hipparcos catalog stars were reprojected into the images. The residuals between our detected star centroids and the expected star reprojections were computed. See Fig. 3. The prototype ODIN camera does not appear to suffer much from radial or tangential distortion, and seems very nearly follows perfect perspective projection without any correction. Nevertheless, since even small errors affect OPNAV performance, correcting for these distortions is still helpful.

[†]Autonomous star identification with unknown focal length is possible, but was neither necessary nor the focus of this field test.

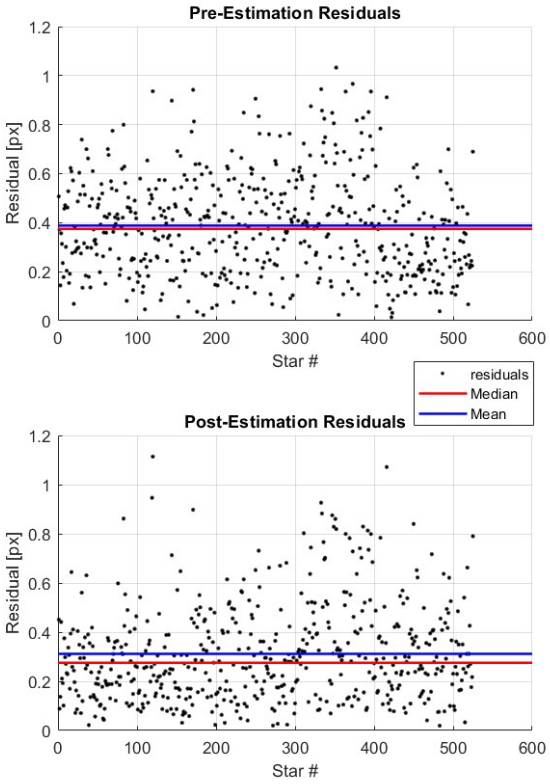

Figure 3. The residuals between all of the identified stars in the 15 star field images and their projected catalog counterparts, before and after the Brown-Conrady distortion fit and focal length estimation.

Horizon Based Position Estimation. The ODIN horizon-based OPNAV approach was tested on a set of 15 images of the Moon. For each image, the direction of illumination in the image was manually estimated (since no attitude estimate was available) and used to complete an image scan to detect horizon points, as shown in Fig. 4. This scan produces coarse horizon points, which were used to generate the initial estimate of the Moon's position.

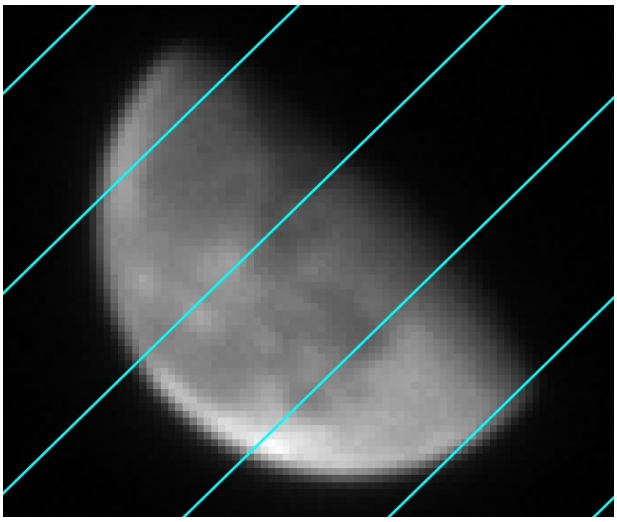

Figure 4. Parallel lines are created in the image, along which a scan is complete to find a significant increase in brightness which is connected to an extended body.

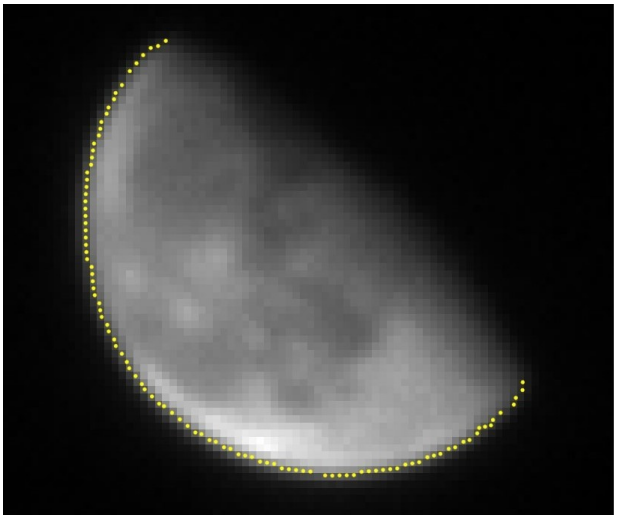

Figure 5. Horizon edge points found after the coarse image scan and refinement via Zernike moments.

These coarse points are then refined to sub-pixel accuracy using the initial estimate and the Zernike moment method.[13] An example of a set of sub-pixel horizon points detected on one of the Moon images is shown in Fig. 5. The refined horizon points are then used to re-solve the CRA for an improved estimate of the Moon's position in the camera frame.

This experiment met the field test's objective of evaluating the camera's ability to generate position estimates using horizon-based OPNAV methods. However, given the single camera set up, no simultaneous estimate of attitude could be made with confidence to transform the position estimate from the camera frame to the inertial frame. Therefore, the true and estimated position vectors could not be directly compared, even though the test site's position was well-known (via GPS). However, since range is invariant to attitude transformations, we may compare the true and estimated distances (i.e., magnitude of the position vectors). The truth position was extracted for the Moon relative to the Earth $\boldsymbol{r}_{em}$ from SPICE ephemeris data[22] (kernel DE440) and using the camera truth position $\boldsymbol{r}_{rc}$ obtained from GPS data, the true range was simply computed as

$$r_{cm} = ||\boldsymbol{r}_{em} - \boldsymbol{r}_{ec}|| \tag{7}$$

The estimated range is simply the norm of the estimated Moon's position from the CRA. The residuals for the estimates from each image was computed, and are shown in Fig. 6. The statistics of these residuals over all 15 images are shown in Table 3.

Table 3. Range from the estimated Moon position is compared to the true range.

	Mean Residual (km)	Median Residual (km)	Mean Percent Error (%)
Coarse	-3250.3	-2708.0	0.8876
Sub-Pixel	-1037.7	-999.11	0.2834

Future Work. Now that an initial test of the hardware and algorithms is complete, future research will work towards a full demonstration of the ODIN concept. This demonstration will be operated from the ground with the horizon-based position estimation working on images the Moon. We anticipate a design consisting of two fisheye lens cameras (with FOVs of $\sim$ 180 degrees) and two narrow FOV cameras (with FOVs of $\sim$ 20 degrees). The instrument will be commanded by a flight computer equivalent, which will run a continuous, autonomous flight software application.

References.

[1] S. Synnott, A. Donegan, J. Riedel, and J. Stuve, "Interplanetary Optical Navigation: Voyager Uranus Encounter," in *AIAA/AAS Astrodynamics Conference*, AIAA 86-2113, 1986.

[2] S. Gillam, W. Owen, A. Vaughan, T. Wang, J. Costello, R. Jacobson, D. Bluhm, J. Pojman, and R. Ionasescu, "Optical Navigation for the Cassini/Huygens Mission," in *AAS/AIAA Astrodynamics Specialist Conference*, AAS 07-252, 2007.

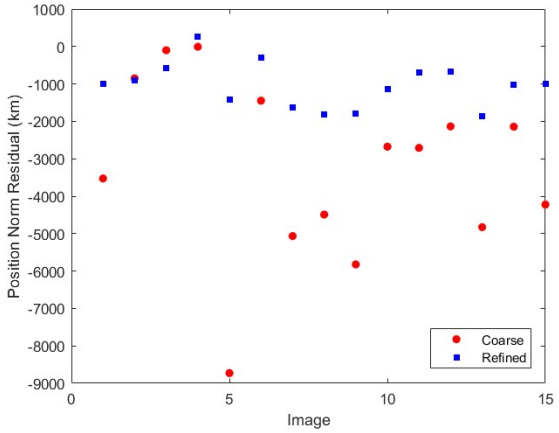

Figure 6. Range residuals between the estimated and true Moon range from the camera. Residuals from both the estimate using the coarse horizon points and the refined horizon points are shown.

[3] W. M. Owen, P. J. Dumont, and C. D. Jackman, "Optical Navigation Preparations for New Horizons Pluto Flyby," in *23rd International Symposium on Space Flight Dynamics (ISSFD)*, 2012.

[4] R. W. Gaskell and et al., "Characterizing and navigating small bodies with imaging data," *Meteoritics & Planetary Science*, vol. 43, no. 6, pp. 1049–1061, 2008.

[5] S. Bhaskaran, J. Riedel, B. Kennedy, and T. chan Wang, "Navigation of the deep space 1 spacecraft at borrelly," *AIAA/AAS Astrodynamics Specialist Conference and Exhibit*, 2002.

[6] R. Inman, G. Holt, J. Christian, K. W. Smith, and C. D'Souza, *Artemis I Optical Navigation System Performance*.

[7] R. D. Olds, C. J. Miller, C. D. Norman, C. E. Mario, K. Berry, E. Palmer, O. S. Barnouin, M. G. Daly, J. R. Weirich, J. A. Seabrook, C. A. Bennett, D. Lorenz, B. Rizk, B. J. Bos, and D. S. Lauretta, "The use of digital terrain models for natural feature tracking at asteroid bennu," *The Planetary Science Journal*, 2022.

[8] D. Scaramuzza, A. Martinelli, and R. Siegwart, "A toolbox for easily calibrating omnidirectional cameras," in *2006 IEEE/RSJ International Conference on Intelligent Robots and Systems*, pp. 5695–5701, 2006.

[9] B. B. Spratling and D. Mortari, "A survey on star identification algorithms," *Algorithms*, vol. 2, no. 1, pp. 93–107, 2009.

[10] J. A. Christian and J. L. Crassidis, "Star identification and attitude determination with projective cameras," *IEEE Access*, vol. 9, pp. 25768–25794, 2021.

[11] G. Wahba, "A least square estimate of satellite attitude," *SIAM Review*, vol. 7, no. 3, p. 409, 1965.

[12] J. A. Christian, "Accurate planetary limb localization for image-based spacecraft navigation," *Journal of Spacecraft and Rockets*, vol. 54, no. 3, pp. 708–730, 2017.

[13] D. T. Renshaw and J. A. Christian, "Subpixel localization of isolated edges and streaks in digital images," *Journal of Imaging*, vol. 6, no. 5, p. 33, 2020.

[14] J. A. Christian, "A tutorial on horizon-based optical navigation and attitude determination with space imaging systems," *IEEE Access*, vol. 9, pp. 19819–19853, 2021.

[15] J. A. Christian, L. Behnacine, J. Hikes, and C. D'Souza, "Geometric Calibration of the Orion Optical Navigation Camera using Star Field Images," *Journal of the Astronautical Sciences*, vol. 63, pp. 335–353, 2016.

[16] M. Krause, A. Thrasher, P. Soni, L. Smego, R. Isaac, J. Nolan, M. Pledger, E. G. Lightsey, W. J. Ready, and J. Christian, "Lonestar: The lunar flashlight optical navigation experiment," *The Journal of the Astronautical Sciences*, 2024.

[17] A. C. Thrasher, M. Krause, S. Henry, M. Mancini, P. Soni, and J. A. Christian, "SONIC: Software for Optical Navigation and Instrument Calibration," *The Journal of Open Source Software*, vol. 9, no. 101, 2024.

[18] M. a. C. Perryman, L. Lindegren, J. Kovalevsky, E. Høg, U. Bastian, P. L. Bernacca, M. Crézé, F. Donati, M. Grenon, M. Grewing, F. van Leeuwen, H. van Der Marel, F. Mignard, C. A. Murray, R. S. Le Poole, H. Schrijver, C. Turon, F. Arenou, M. Froeschlé, and C. S. Petersen, "The hipparcos catalogue," *Astronomy and Astrophysics - A&A*, vol. 323, no. 1, pp. 49–52, 1997.

[19] D. Mortari, M. Samaan, C. Bruccoleri, and J. Junkins, "The pyramid star identification technique," *Navigation: Journal of The Institute of Navigation*, vol. 51, no. 3, pp. 171–183, 2004.

[20] A. E. Conrady, "Decentred lens-systems," *Monthly Notices of the Royal Astronomical Society*, vol. 79, pp. 384–390, 03 1919.

[21] D. Brown, "Close-range camera calibration," 1971.

[22] R. S. Park, W. M. Folkner, J. G. Williams, and D. H. Boggs, "The jpl planetary and lunar ephemerides de440 and de441," *The Astronomical Journal*, vol. 161, p. 105, feb 2021.